Protecting and stimulating effect on the degradation of eosin lakes. Part 1 : lead white and cobalt blue

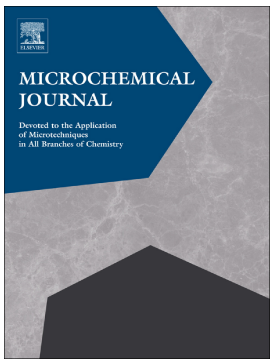

Protecting and stimulating effect on the degradation of eosin lakes. Part 1: Lead white and cobalt blue

Alba Alvarez-Martin, Koen Janssens

PII: S0026-265X(17)30855-X
DOI: doi:10.1016/j.microc.2018.05.005
Reference: MICROC 3153

To appear in: *Microchemical Journal*

Received date: 1 September 2017
Revised date: 4 May 2018
Accepted date: 4 May 2018

Please cite this article as: Alba Alvarez-Martin, Koen Janssens , Protecting and stimulating effect on the degradation of eosin lakes. Part 1: Lead white and cobalt blue. The address for the corresponding author was captured as affiliation for all authors. Please check if appropriate. Microc(2017), doi:10.1016/j.microc.2018.05.005

Protecting and stimulating effect on the degradation of eosin lakes. Part 1: Lead white and Cobalt blue

Alba Alvarez-Martin* and Koen Janssens

AXES, Department of Chemistry, University of Antwerp, Groenenborgerlaan 171, 2020 Antwerp, Belgium

*Corresponding author E-mail address: alba.alvarez@usal.es

Keywords: Eosin lakes, Color fading, FTIR-ATR, Raman spectroscopy, UV-VIS spectroscopy, SEM-EDX

Abstract

An important problem encountered during the preservation of paintings and other artworks is the fading of the original colors due to exposure of the colorants to light. This fact is clearly evidenced in some of Vincent Van Gogh's paintings in which an organic red, eosin or geranium lake, is present.

The identification of eosin and the characterization of its degradation products in paintings represents a challenge because of (i) the generally low concentration of the pigment remaining after an aging period of ca 100 years, (ii) the scarcity of the paint micro samples available for analysis and the difficulty of obtaining additional ones and (iii) the complexity of the degradation behavior of eosin when it is mixed with organic or inorganic pigments, binding media or varnish.

This study presents an accelerated ageing experiment of eosin paint models in order to understand better the discoloration process; more specifically the influence of different metals with which eosin forms complexes and of the presence of admixture pigments such as lead white and cobalt blue on the lightfastness of eosin is evaluated. Paint model samples were prepared using eosin, lead white, and cobalt blue in different mixing ratios and were characterized with several techniques before and after ageing. The possible formation of intermediate molecular forms during the ageing experiment and the influence of pigment ratios on the discoloration process were monitored at periodic intervals using a combination of UV-Visible and attenuated total Reflectance-Fourier transform infrared (ATR-FTIR) spectroscopies. Raman spectroscopy, scanning electron microscopy coupled to energy-dispersive X-ray analysis (SEM-EDX) and optical microscopy (OM) analyses were performed to gain information about the discoloration processes taking place within the paint models.

Eosin precipitated on lead, aluminum and potassium/aluminum salts was used. These three lakes showed similar discoloration rates under light exposure. In contrast, the presence and relative abundance of the admixture pigments lead white and cobalt blue had a significant influence on the (speed of the) eosin discoloration process. The presence of lead white and cobalt blue appears to stimulate the eosin degradation. However, the cobalt blue shows less influence in the discoloration process, showing a protective effect during the first stages of the aging. This may be qualitatively explained in terms of the ability of lead white to scatter light towards eosin molecules and the absorption characteristics of cobalt blue in the green range of the electromagnetic spectrum, shielding eosin from incoming light.

The color changes observed in the paint reconstructions are similar to discoloration phenomena visible in some Van Gogh paintings and can offer an explanation of the gradual discoloration

process that took place over the years. These insights will be helpful to estimate the original hues color used/intended by the artist.

1. Introduction

The palette of Vincent Van Gogh is well known nowadays thanks to numerous studies carried out by conservators, historians and scientists. The degradation process and reactivity of inorganic pigments such as lead [1], chromium [2] and cadmium-based [3] compounds have been deeply studied in the last few years. The analysis of the state of degradation of inorganic pigments is possible by using a combination of several techniques such as X-ray diffraction (XRD) and X-ray fluorescence (XRF) [4]. On the other hand, the characterization of organic pigments in many cases is more complex due to their lower stability compared to the inorganic compounds, and requires a combination of chromatography, mass spectrometric techniques and a range of vibrational spectroscopic techniques [5-8]. The identification and characterization of organic pigments in paintings is rendered even more difficult because organic lakes are often light sensitive materials [9,10].

Organic red colorants such as eosin, cochineal, methyl violet, Kopp's purpurin, madder redwood and brazilwood [11,12] were progressively used by Vincent Van Gogh in the second half of his career (1885-1891). Most of these red lakes mentioned above have been identified in paintings from the period that the artist spent in Antwerp and Paris (1885-1888). However, it was not until his stay in Arles (1888) that Van Gogh started to also include eosin (sometimes called geranium lake) in his red palette [13]. While he wrote to his brother about the marked tendency of eosin to fade upon light exposure [13,14], it is possible that he did not have the opportunity to fully

appreciate the significant effect the discoloration of eosin would have on the overall outlook of the paintings he used it in, since he only used eosin in the last two years of his career.

In general, organic lakes can be obtained by precipitating a soluble organic dye onto an inorganic substrate (mostly a metallic salt) yielding a solid pigment powder. In these solids, the eosin molecules are present as complexes with metal ions. Geranium lake offers a wide variety of possible hues ranging from an orange-scarlet to bluish-red, one of the defining factors being the chelating metal. Trace analysis of some painting fragments have revealed different metal compositions of the lakes, suggesting that the geranium lake used by Van Gogh may have come from different manufacturers [11]. Geranium lake was almost never used in pure form; it was commonly mixed with other pigments or glazed over them. It was reported that Van Gogh used to frequently employ geranium lake mixed with blue or green pigments to obtain a final hue ranging from pale, middle of deep tones or purple and brown [11]. In the same way, paler tints of red and pink were also obtained by the artist by mixing eosin with varying amount of white pigments.

In addition, the stability of organic pigments can be influenced by the substrate/metal ion used in the synthesis [15], the binding medium of the paint [16] and the other pigments present in it [17]. The photochemistry behavior of eosin in solution has been previously studied, suggesting the formation of photo-excited forms [18-20]. However, these intermediate states described in the bibliography have not yet been identified in oil based medium. Assessing the extent of eosin discoloration in a specific location in a work of art is problematic since there generally are no detailed records of the original color of the paint mixture as prepared by the artist. For this purpose, the creation of a reference collection of reconstructed geranium lakes is a crucial step towards understanding the discoloration process that the lakes undergo over the time. The paint

models serve a double function: first, to permit to reproduce the original hues corresponding to historical recipes/procedures. Second, to support a better interpretation of the analytical results obtained from the analyses of paintings from the end of the 19th/beginning of 20th century [21].

The reproduction of the synthesis of eosin lakes is rendered difficult by the scarcity of the literature on this topic. In a recent study, monometallic and historical bimetallic eosin lakes were synthesized and characterized by mass spectrometry, attenuated total reflection Fourier transform infrared (ATR-FTIR) and nuclear magnetic resonance (NMR) [22]. According to Anselmi et al., monometallic eosin lakes (Eo-M) can show variously anchored states based upon the metal (M) bonded to the eosin molecule (via the xanthene moiety or the isolated ring present in the structure), always with a 2:1 (Eo:M) ratio with the carboxylic group coordinating the metal. Two main anchored species have been distinguished: (i) eosin lakes based on M = Al^{3+}-ions, featuring a bridged bidentate anchor and (ii) eosin lakes complexed to M = Pb^{2+}-substrates, that present a H-bonded complex.

Several studies have been focused on the fugitive behavior of geranium lake [11,14,23], but to our knowledge, there are no reports in the literature on how the degradation of Eo-M is influenced on the one hand by the nature of the metal and on the other hand by the presence of other pigments in the paint. These two topics are addressed in this paper.

To this effect, three types of geranium lakes were synthesized by the precipitation of the organic dye with three different metallic salts, followed by the paint models preparation. The latter was done by mixing one of the Eo-M lakes with lead white and cobalt blue in different ratios. Lead white was selected as one of the admixture pigments as it was among the most commonly used white pigments in many historic periods and is still in use today. The other pigment, Cobalt blue, is encountered for the first time in Van Gogh's Parisian paintings (1887) after his stay in

Antwerp; and he continued using it until the end of his life [11,24]. Samples were prepared in linseed oil in order to be as most accurate as possible to the historical oil paints described in the literature [10,11,14]. The paint reconstructions were aged by exposure to the solar emission spectrum and then analyzed by OM, SEM-EDX, FTIR-ATR, Raman and UV-VIS spectroscopy to assess whether or not the different mixtures can affect the discoloration process.

2. Materials and methods

2.1. Synthesis of Eosin lakes

Eo-M lakes based on eosin-Y (99% Sigma-Aldrich) (Fig. S1) and different coordinating metal ions (M=Al^{3+}, K^{+}/Al^{3+} and Pb^{2+}) were prepared with aluminum chloride hexahydrate ($AlCl_3 \cdot 6H_2O$) (Fluka), aluminum potassium sulphate dodecahydrate ($KAl(SO_4)_2 \cdot 12H_2O$) (Sigma-Aldrich) or lead (II) acetate trihydrate ($Pb(CH_3CO_2)_2 \cdot 3H_2O$) (Merck). The synthesis of the lakes was carried out according to the protocol proposed by Claro et al. [25]. The lakes (denoted below as Eo-Al, Eo-Al/K and Eo-Pb, respectively) showed different colors, varying from reddish to purple. Recently, it was shown that there is not a clear correlation between the coordination metal and the final color; rather, the experimental pH and the reaction conditions (also) appear to be among the main factors that determine the final hue of the lake [22].

2.2. Paint sample reconstructions

Cobalt blue (#45710) was supplied by Kremer (Kremer Pigmente GmbH & Co. KG). Lead white was synthetized “in house” on a small scale following the Dutch stack process [26]. The bleached linseed oil (Talents, NL) employed was diluted with turpentine. This type of oil shows less tendency to yellow than the normal linseed oil and is recommended when is used in combination with whites, pale colors, and light blues.

Paint reconstructions were prepared starting from either Eo-Al, Eo-Al/K or Eo-Pb; three different sets of mockup paints were prepared by (a) mixing one Eosin lake type with lead white and/or cobalt blue in different ratios, yielding paints with hues ranging from light pink to dark red and from purple to dark brown. Table 1 shows the different ratios used to prepare the paints. The pigments were prepared with a glass muller using bleached linseed oil. To obtain a suitable paint consistency the amount of oil was between 30-40 mg in all samples, the total paint mass prepared being around 200 mg. The final paint mixtures were applied as homogeneous layers onto acrylic glass and allowed to dry for 3 weeks at low light levels at 20 °C and at environmental humidity (about 60% RH). A duplicate set of samples was placed in the dark to act as a color reference. In addition, samples containing only CB and LW in different ratios were studied as a color reference. A total of 143 paint samples were analyzed in this study.

2.3. Light ageing experiment

Paints were light-aged in a solar box (Solarbox 1500e, Climatronix). The UV light source was a xenon lamp which provides radiation with wavelengths between 300 nm and 800 nm. The temperature and irradiance were 60 ºC and 550 Wm^{-2}. No active control of the relative humidity (RH) was possible in the aging chamber employed. Paints were irradiated for 192 h.

Table 1. Preparation of paint reconstructions for M = Al, Al/K and Pb.

Sample series	Sample code	Eo-M: LW: CB relative mass abundance
all	1	10:0:0
I	2	10:0:1
I	3	10:0:2.5
I	4	10:0:5
I	5	10:0:7.5

II	6	1:10:0
II	7	2.5:10:0
II	8	5:10:0
II	9	7.5:10:0
III	10	1:10:1
III	11	1:10:2.5
III	12	1:10:5
III	13	1:10:7.5
III	14	1:10:10
IV	15	1:16:10
IV	16	1:16:5
IV	17	1:16:2.5
V	18	10:10:7.5
V	19	10:6:7.5
V	20	10:4:7.5
V	21	10:2:7.5

Eo: eosin; LW: lead white; CB: cobalt blue.

2.4. Color measurement (CIELAB)

Color changes were recorded at different times (0, 12, 24, 48, 60, 72, 96, 144 and 192 h) during the ageing process, using an AvaSpec 2048-SPU spectrophotometer (Avantes, UK). The spectrophotometer is controlled by a PC with the AvaSoft 7.5.3 software. Spectral-reflectance data was collected from 200 to 800 nm at 10 nm intervals for the standard D65 daylight illuminant and 2^{o} observer angle with specular reflectance included. An average of six measurements recorded directly in each paint sample was used for the calculations. The values of the chromatic coordinates (a*, b*) and luminosity (L*) were provided by the software and the overall change in color (ΔE*) was calculated by means of the CIE 1976 (L*a*b*) formula, $\Delta E^* = [(\Delta L^*)^2 + (\Delta a^*)^2 + (\Delta b^*)^2]^{1/2}$ [27]. Here, ΔL* represents the difference in lightness/darkness on

a scale from black to white (0-100), Δa* the redness/greenness and Δb* the yellowness/blueness. The shift of the chromatic coordinates obtained for all the aged samples, before and after the accelerated ageing treatment were calculated using the relation $\Delta x^* = x^*_{unaged} - x^*_{aged}$.

2.5. Infrared spectroscopy (FTIR-ATR)

FTIR-ATR analyses were performed on all samples before and after the ageing treatment in order to detect changes in the paint samples. For this purpose, a small paint chip was collected from the corner of the paint models. The resulting spectra was recorded on a Platinum Diamond-ATR ALPHA-spectrometer (Bruker, USA). The spectrophotometer is directly controlled by a PC with the OPUS software from Bruker Optics. All the spectra were registered from 4000 to 400 cm^{-1}, at 4 cm^{-1} spectral resolution and with 24 scans. The spectral background was reordered prior to collection of each spectrum.

2.6. Optical Microscope (OM)

A selection of 10 micro samples taken from the paint models, before and after the ageing experiment, were mounted in a high viscosity acrylic resin (ClaroCit, Struers Inc., Cleveland, OH), the cross section was polished until a smooth surface was obtained. Images of the sectioned samples were acquired on a Leica DMI5000 M microscope coupled to a Leica DFC450 camera.

2.7. Scanning electron microscopy (SEM-EDX)

A Field Emission Gun-Environmental SEM-EDX (FEG-ESEM-EDX, FEI Quanta 250) was used to inspect the surface of the paint cross sections with the aim of determining the distribution of bromine along the selected cross section after light exposure. Secondary Electron (SE) images, X-ray spectra and element maps were collected using an accelerating voltage of 20 kV. The X-ray take-off angle was 30°, the working distance 10 mm, the current differed between 0.2 and 6 nA and the chamber pressure is 10^{-4} Pa.

2.8. µ-Raman spectroscopy

Raman spectra were collected with an inVia spectrometer (Renishaw PTY Ltd.). Samples excitation were performed by means of a green laser (514.5 nm) or a red laser (785 nm) and using a Leica N Plan long-working-distance objective (x50/0.5), resulting in a laser spot of ± 1.2 µm. The grating was calibrated using the 520 cm^{-1} silicon band. The density of the grating was 1800 and 1200 lines/mm for the green and red laser respectively. The spectral resolution is <1cm^{-1} (according to the manufacturer). Exposure time, number of acquisitions and laser power for the red were 15 s, 10 and 0.27 mW and for the green laser were 15 s, 10 and 0.04-0.32 mW. Raman signals were detected by a Peltier cooler CCD detector. An optical microscope was used to focus the laser on the sample.

3. Results and Discussion

3.1. Microscopy Analysis

Samples taken from the (un)degraded paint models were examined as cross sections with optical and scanning electron microscopy. The cross-sections shown in Fig. 1 belong to five Eo-Pb-based mixtures before and after ageing.

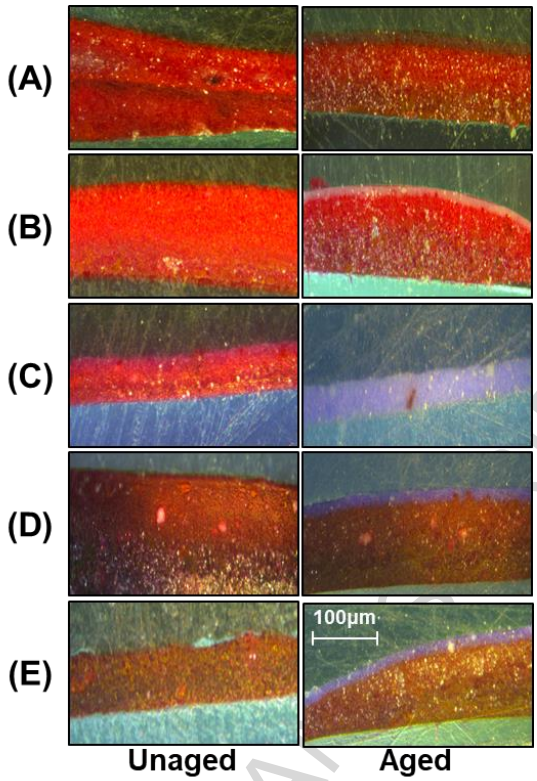

Fig. 1. Optical microscopy of resin-embedded paint cross sections before (left) and after (right) ageing. UV illumination from the top in all cases. The samples (A-E) correspond to five paint models containing different mass ratios of Eo-Pb, lead white and cobalt blue. (A) 10:0:0; (B) 7.5:10:0; (C) 1:10:1; (D) 10:0:7.5; (E) 10:10:7.5.

After UV illumination, no significant difference between the unaged and aged samples containing only eosin are visible (resp. left and right image in Fig. 1A). Nevertheless, when eosin is mixed with lead white or cobalt blue, the top layer shows a marked discoloration of the original color; this is clearly visible in Figs. 1B-E. For example, as seen in Fig. 1C, the originally red/purple tinted lead white/cobalt blue mixture (left image) almost completely turns light mauve (right image).

In both Figs. 1B (Eo-Pb/LW mixture without CB) and 1E (same mixture, but with 7.5% CB), a clear discoloration on the top layer is visible, next to a less pronounced color change throughout the aged sample. When the relative amount of lead white in the mixture is increased, an increase in the thickness of the degradation layer is also noticeable. In the case of the paint model with the highest mass ratio of lead white (Fig. 1C), a total fading of the eosin along the paint model is clearly observed, with the exception of a red (Eo-Pb) grain near the bottom of the sample. Comparing Figs. 1D to 1A allows to qualitatively assess the effect of the presence of cobalt blue on the discoloration process. When cobalt blue is present in the paint reconstruction (Fig 1D), a less pronounced color change after light exposure is perceived. The discoloration is observed only in the upper few micrometers of the paint and no color changes are observed in the rest of the sample. The same effect is visible in Fig. 1E, where the paint discoloration at greater depth is also less pronounced compared to Fig. 1B.

The results observed are corroborated by previous analyses of Van Gogh paintings, where the presence of blue pigments, such as cobalt blue or Prussian blue, appears to preserve the light-induced degradation of eosin [11].

In view of the fact that the optical photographs of Fig. 1 in many cases show a significant loss of superficial red color, the same cross-sectioned samples were examined by means of SEM-EDX in order to verify whether the color loss could be associated with a modification of the microscopic Br distribution, a marker for the presence of (remains of) the eosin molecules. However, these SEM-EDX analyses revealed no such relation at all (Fig. S2). The SEM-EDX data indicated that the discoloration is likely due to the breakdown of the chromophore moiety [28,29], where the Br stays immobilized in the paint, and is presumably still attached to a large extent to the remains of the molecule or to the oil media. These results are consistent with the

fact that Br has been detected in Van Gogh paintings by means of Macroscopic X-ray fluorescence analysis in those areas where (faded) eosin lake has been identified [11,30,31] by other methods.

3.2. Colorimetric measures

Figs. 2 and S3-4 show the appearance of the surface of the paint mockups before and after exposure to UV light. Specific color differences can be observed: violet mixtures fade to blue; brown mixtures become purple, while intense pink mixtures turn pale. These changes may be associated with the loss of the red colorant - the extent to which these take place is influenced by (a) the abundance of eosin and (b) the presence of other pigments in the mixture.

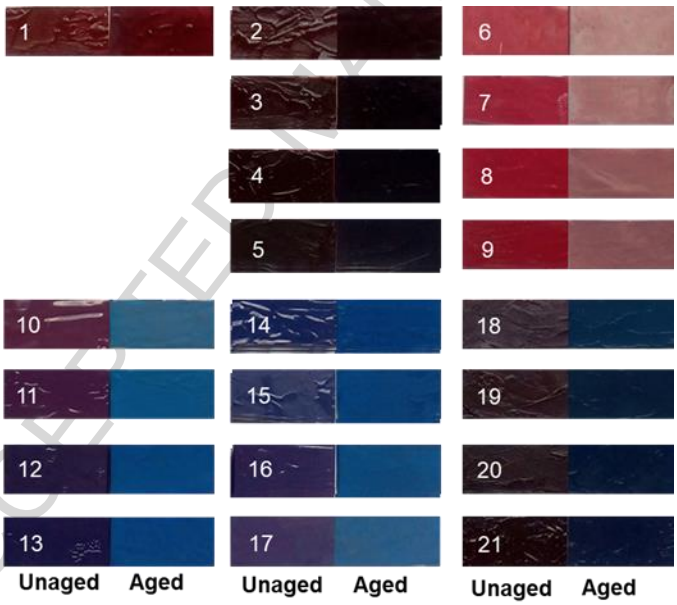

Fig. 2. Optical photographs of the surface of Eo-Al paint models before (left) and after (right) ageing. Numbers correspond to the sample codes given in Table 1. (For comparison, equivalent images for the Eo-Pb and Eo-Al/K paint models are included in Fig. S3-4).

In order to evaluate any dependence of the aging time on the discoloration process, a total of nine color measurements were performed during the ageing period after 0, 12, 24, 48, 60, 72, 96, 144 and 192 hours of light exposure. Control samples were also evaluated at the beginning of the experiment and five months later in order to detect any modification due to natural ageing; however, no color changes were detected (data not shown). These results suggest that, without light, temperature and relativity humidity do not have a significant influence on the color change of eosin.

It is interesting to point out that the total color change (ΔE*) presented for all the aged samples was larger than 1, indicating that the changes are visible to the human eye.

The results presented below deal in first place, with the influence of the metal coordinated to the eosin molecules on their light-stability and in second place, are concerned with the effect of the other pigments present in the paint model mixtures.

3.2.1. Influence of the metal complexed to eosin

Fig. S5 shows a CIELAB diagram in which it can clearly be observed that paint samples containing only eosin show a shift in the yellow component; in this case the red coordinate remained unchanged during the light exposure. Fig 3. summarizes the total color change (ΔE*) as a function of aging and intercompares the behavior of Eo-Al, Eo-Al/K and Eo-Pb. The total color change of paint models that only contain eosin lakes (Fig. 3A) remained constant as a function of aging time, while no significant differences were observed among the three Eo-M types. The recorded ΔE* values, of the lakes where only eosin is present, are also the lowest observed; larger values are obtained when cobalt blue or lead white were present in the mixtures (Fig. 3. B-F). This indicates a higher stability of the pigment when it is present by itself in the paint and confirms that other pigments can measurably influence its stability.

In general, Eo-Pb and Eo-Al/K appear to be more light-sensitive than Eo-Al. This variation in lightfastness can be directly related to the difference in the manner in which the metals are coordinated: as observed by Anselmi et al. [22], eosin is complexed with aluminum only at one site for each molecule where the charge is probably localized on the metal; however, in the case of lead, a double anchoring, between both oxygen atoms of the carboxylic group is in place, suggesting that the charge is localized on the xanthene moiety. This electronic differences along the complexes described by Anselmi et al. may suggest the main cause of the differences in their photochemical stability. The difference in degradation behavior between Eo-Al and Eo-Al/K is consistent with the observation by Saunders and Kirby [32] for other organic lakes coordinated to mixtures of metals. In such “mixed metal” cases, they describe the chemical bonding between the dyestuff molecule and the aluminum as less strong than in “single metal” Eo-Al lakes, where the aluminum is the only coordination metal.

Since the effect of the metal (M) on the degradation behavior of Eo-M is rather limited, the influence of the admixture pigments lead white and cobalt blue on the discoloration process will be explained in the next sections without making any distinction between the complex metals.

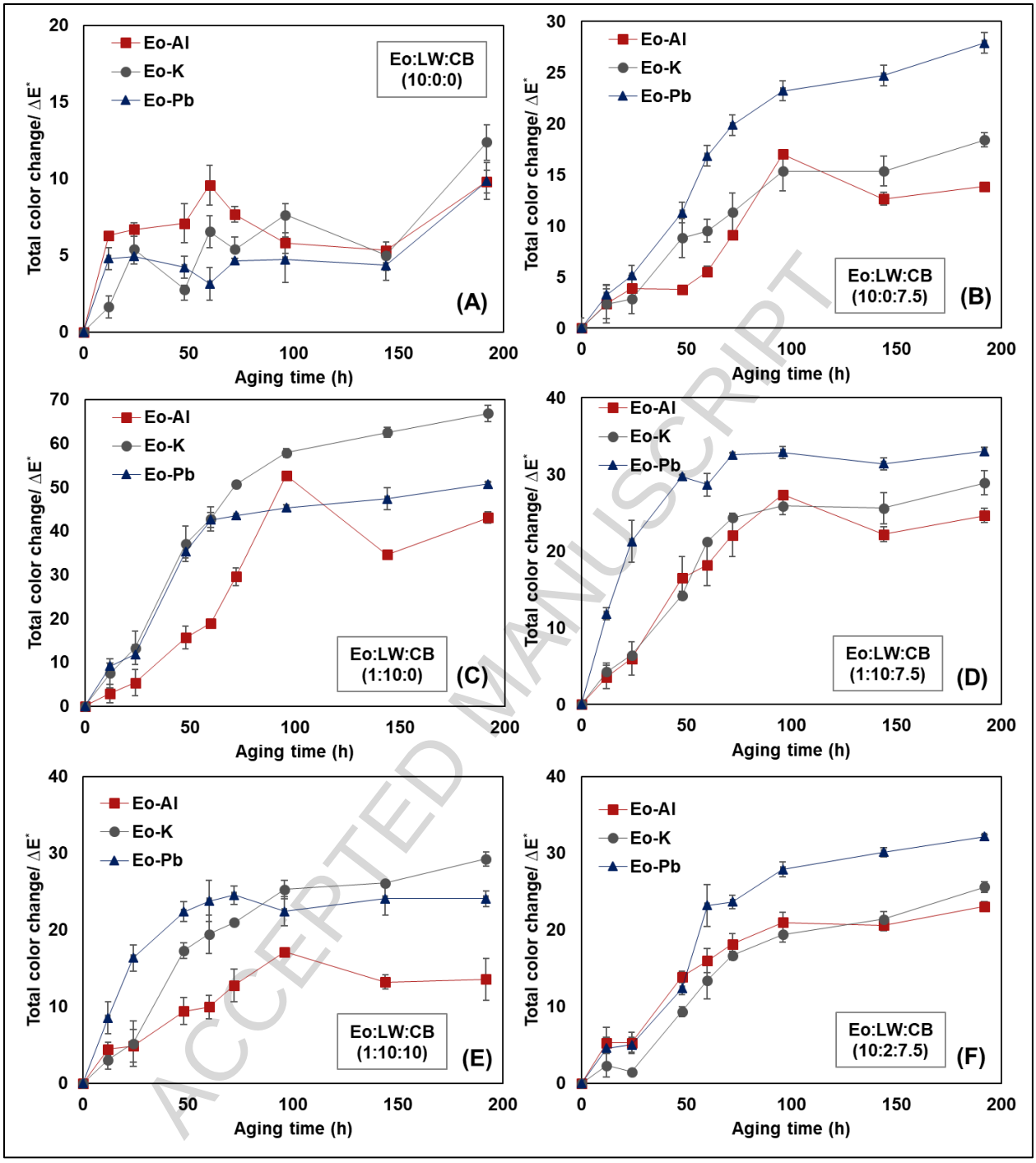

Fig. 3. Comparison of influence of the complex metal (Al, Pb or Al/K) in the total color change, measured in units of ΔE*, against aging time. **(A)** Paint models containing only Eo-M; **(B)** paint models containing mixtures of Eo-M and CB; **(C)** Paint models containing mixtures of Eo-M and LW. **(E-F)** ternary Eo-M, LW and CB mixtures.

3.2.2. Influence of Lead white in binary Eosin-LW mixtures

Fig. 4A and C show the CIELAB diagram and the total color change for the paint models obtained from different Eo-Al/K and LW mixtures. All paint models analyzed in this set showed a decrease in both components (redness and yellowness) from the beginning of the experiment, but the loss of the red (a*) proceeds more rapidly than the yellow component (b*). This may suggest that any intermediates or degradation products formed during the process are degraded faster than the yellow components. However, in the paint samples with a higher lead white abundance (in which the eosin is thus most diluted), the decrease of the red component is faster than for the samples in which less lead white is present. Fig. 4C illustrates the fugitive behavior of Eo-Al/K when combined with lead white, where the higher dilution factor in the sample is correlated with an increase in ΔE*. The low decrease of the yellow component in presence of high amount of LW (Fig. 4A, sample (1:10:0)) shows that the decrease of the b* coordinate is not associated with a previous yellowing of the sample.

The more pronounced loss of color in the paint models when lead white is present, may be related to the fact that the impinging radiation is not completely back-reflected by the white pigment at the surface, and the remainder enters the paint layer. In addition, the internal scattering inside the paint might be the cause of the color change along the paint [32,33].

3.2.3. *Influence of Cobalt blue in binary Eosin-CB mixtures*

Fig. 4B shows that Eo-Al/K features a similar degradation behavior regardless of cobalt blue abundance in the paint; the same holds true for Eo-Pb and Eo-Al/K (not shown). All samples show a simultaneous decrease of both color coordinates (a* and b*). For this set of samples, the decrease of the red component was lower than in the mixtures in which lead white is present, indicating that cobalt blue has less impact, on the discoloration of the red lakes, than lead white.

This effect is also noticeable when the total color change is analyzed. The variation of ΔE* when cobalt blue is present ranges between 15 and 24 (Fig. 4D); for the mixtures containing lead white the range is from 40 to 70 ΔE* units (Fig. 4C).

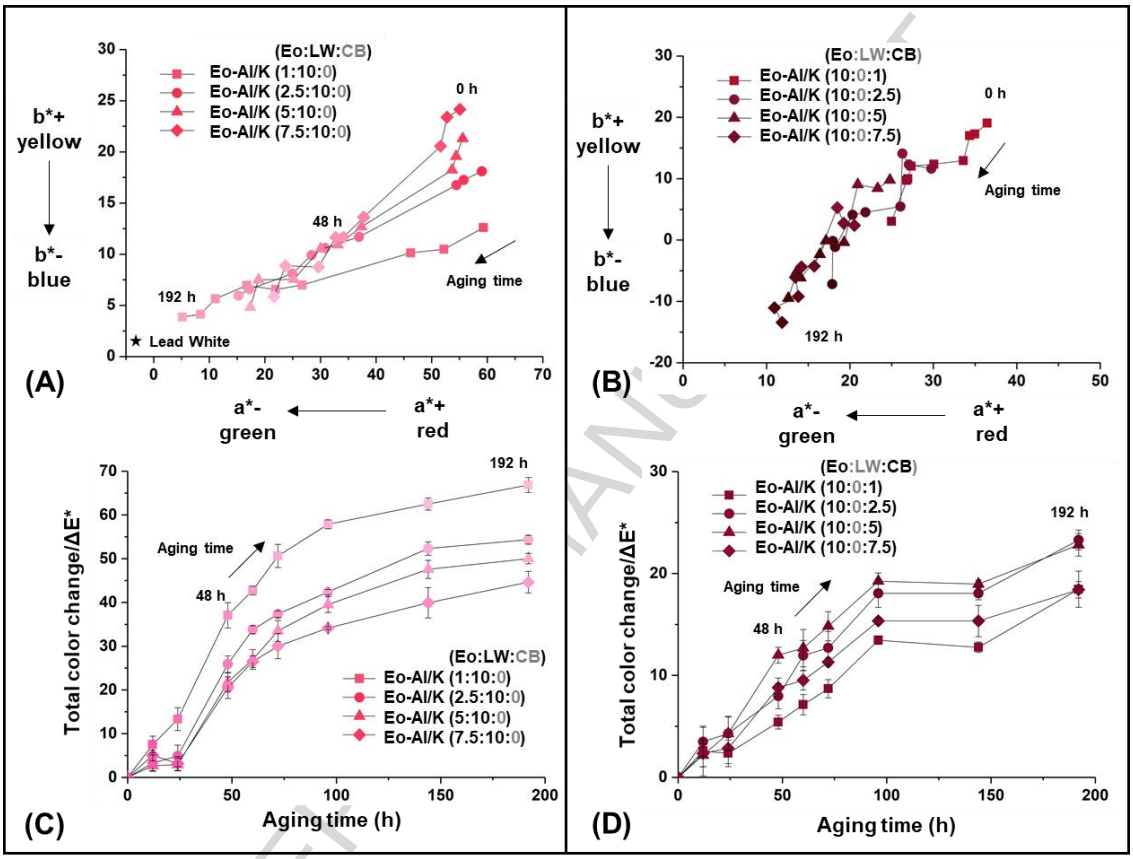

Fig. 4. CIELAB diagrams of paint models consisting of **(A)** Eo-Al/K and lead white and **(B)** Eo-K/Al and cobalt blue mixtures showing changes in redness (a*) and yellowness (b*) during the aging experiment. The color used for the symbols represent the color of each sample during light exposure. **(C)** and **(D)** represent total observed color change of ΔE*, during the aging experiment for the same set of samples. Mixtures based on Eo-Pb and Eo-Al lakes instead of Eo-Al/K showed similar results.

3.2.4. Behavior of ternary mixtures of eosin, lead white and cobalt blue

The CIELAB diagrams (Fig. 5A and B) for the paint models that contain cobalt blue, lead white and Eo-Al or Eo-Pb in different mass ratios, show a loss in the red component associated with a perceptible increase in the yellow component during the first 24 hours under light exposure. After this time the yellow coordinate revealed a decrease throughout the entire experiment. The decrease of the yellow component of the most diluted samples (Fig. 5A) is slower that the red component during the first stages of the aging process. Only after most of the redness has disappeared (after ca 96 h), the yellow component begins to decrease. In this set of samples, the relative abundance of cobalt blue present in the paint is directly related to the decrease in the total color change ΔE^* (Fig. 5C).

The same holds true for the samples with a high relative abundance of cobalt blue (Fig. 5B and D). However, in this case the shift of the yellow component is more prominent than in samples with a low cobalt blue abundance. Similar results have been described [14,32] for other organic lakes such as kermes and cochineal. The tendency of the color change suggests that during the initial stages of the fading process, one or more yellow compounds are generated due to the breakdown of the red component. We consider it plausible that the increase of the yellow component results from the formation of an intermediate breakdown product of eosin. The same phenomenon was observed [34] when alizarin lake was mixed with titanium dioxide. Also here the lake does not immediately fade to a colorless state; and a yellow intermediate was detected via spectroscopic techniques. In addition, the slow decrease of the red component at early stages of the aging experiment may indicate the decrease of the degree debromination [35] in the organic red pigment. The debromination process of eosin in solution has been the subject of

several studies [28,29,36,37]. However, the correlation between the discoloration process and the degree of bromination in eosin lakes requires further study.

When the relative abundance of cobalt blue is high and remains constant, the total color change has the same pattern for all samples, regardless of the amount of lead white present (Fig. 5D). This observation shows that when cobalt blue is abundantly present, the effect of lead white over the discoloration is diminished.

The fact that the blue pigment can slow down or prevent the discoloration process of eosin has been observed in previous studies on Van Gogh paintings. (i) Centeno et al. in their study of *Irises and Roses* [30] found that eosin was protected by a Prussian blue layer. (ii) The comparative analysis of different versions of *The Bedroom* revealed the presence of red lake particles covered by a blue layer, presumably more stable than the red lake on its own [13]. (iii) The analysis of a paint cross section taken from *The Sower* showed the original purplish color in the bottom of the sample, while the top part is blue due to the fading of eosin mixed with blue and white pigments. However, when eosin was mixed with a high proportion of blue pigment as in *Pieta (after Delacroix)* the analysis showed an opaque paint mixture where eosin was detected along the cross section [11].

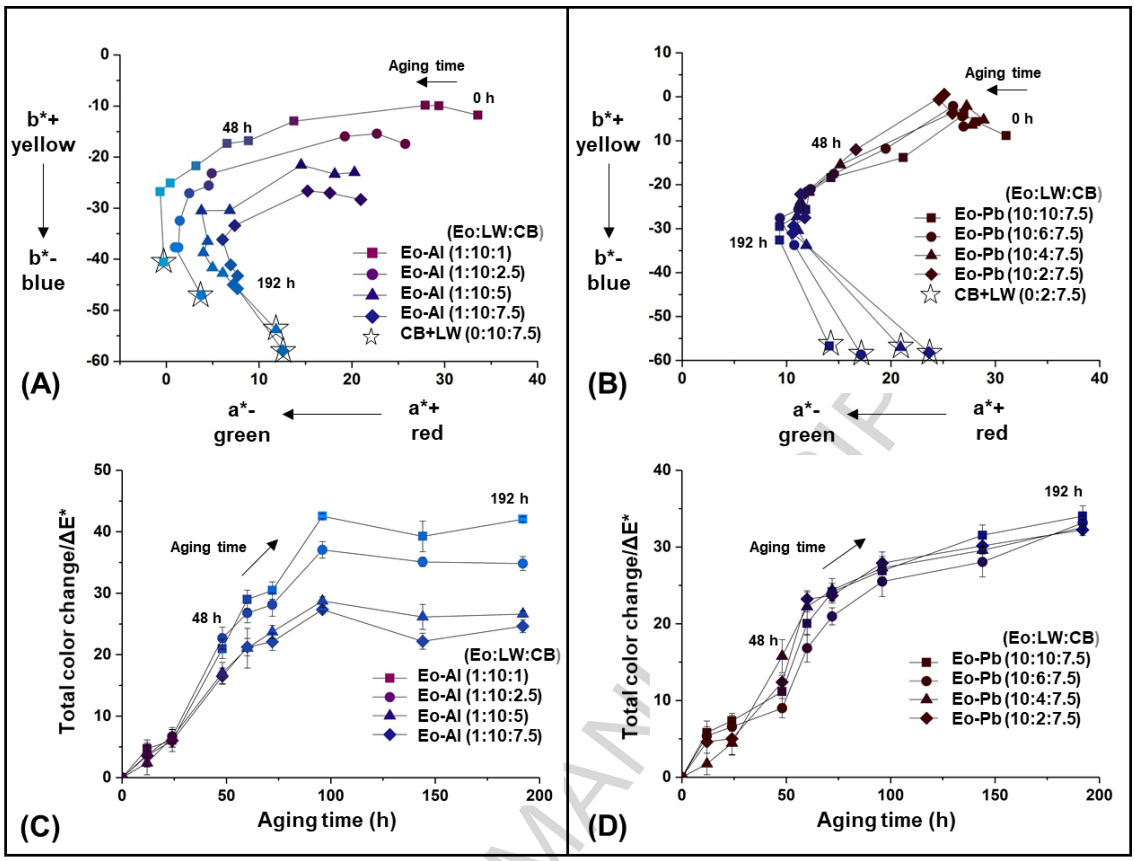

Fig. 5. CIELAB diagrams of paint models containing different mass ratios of Eo-Al or Eo-Pb, lead white and cobalt blue (A) and (B) showing the changes in redness (a*) and yellowness (b*) during the aging experiment. The color used for the symbols represent the color of each sample after light exposure. (C) and (D) represent the total color change ΔE* during the aging experiment for the same set of samples. Mixtures based on Eo-Al/K showed similar results.

3.2.5. *Reflectance*

The reflectance spectra of four representative paint models are shown in Fig. 6A-D. The spectrum of geranium lake (data not shown) appears flat throughout the violet region into the green and features a sharp increase in reflectance at about 600 nm. The characteristic absorption of eosin observed in the visible region is due to n → π* transitions [23]. In the analysis of the

paint model containing Eo-Al/K and lead white (Fig. 6A), the characteristic absorption band of Eo-Al/K is observed even at low concentrations. After aging, the stronger contribution of the absorbance of lead white between 425 and 675 nm is observed [38].

When the paint model contains cobalt blue (Fig. 6B, C and D), the characteristic band around 600 nm associated with the red color is still visible. However, the relative intensity of this band decreases when the cobalt blue abundance increases in the paint, and in all samples this band decreases after the ageing treatment due to the fading of the eosin. Additionally, after aging Fig. 6C and D show a new reflectance band in the blue range with a maximum at 475 nm, characteristic of cobalt blue.

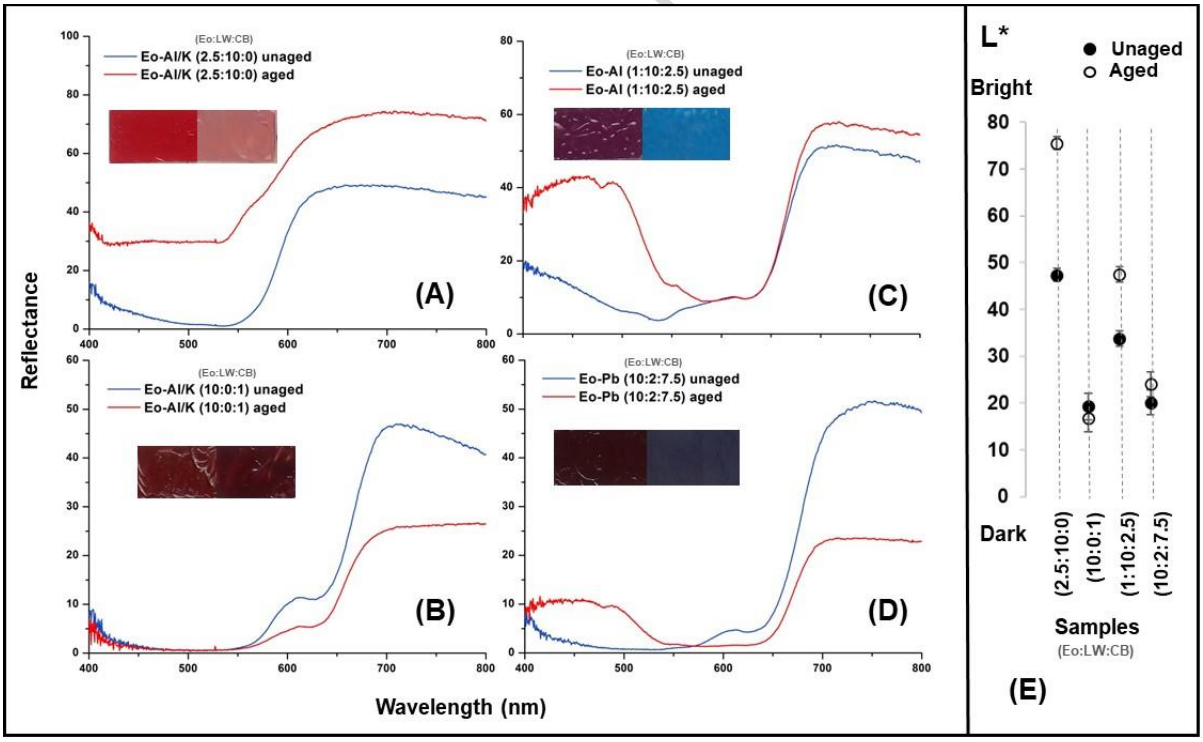

Fig. 6. **(A-D)** Selection of the diffuse reflectance UV-VIS spectra of paint models before and after aging. **(E)** Represents the variation of the L* (lightness/darkness value) for the same samples.

The variation observed in the absorption intensity of the spectra between 610-750 nm (see Fig. 6A-D) is directly related with the brightening or the darkening of the surface of the paint associated with the shift of the L* coordinate (Fig. 6E).

After ageing, Fig. 6B and D show a decrease of the reflectance in the red spectral range (610-750 nm) related to the darkening of the paint as can be observed in the decrease of the L* coordinate ($\Delta L^* < 0$).

Interestingly, samples with a high lead white abundance in the mixture (Fig. 6A and C), feature an increase in the reflectance after aging, correlated with the increases of the L* value after aging, indicating a rise in the overall paint brightness caused by the fading of the original color. When LW is present the large shift in the L* coordinate, in comparison with the samples that contain CB, might be explained by the nature of the LW, which is more transparent than the CB, allowing the light to pass through the paint and stimulating the degradation of eosin. When LW is present in the sample the internal light scattering inside the paint is the main cause of the color change in the underneath layers. Meanwhile, the presence of cobalt blue increases the absorption of light at the surface of the sample, inhibiting the discoloration of eosin located deeper within (Fig. S6). From Fig. 7 it is clear that CB in linseed oil efficiently absorbs radiation in the wavelength range 500-600 nm; as such, CB competes with Eo-Al for the photons in this range. The effect is that the eosin lake molecules in the Eo-Al/CB/linseed mixture are partially shielded from the incoming light of 500-600 nm and thus degrades more slowly than in the situation when CB would not be present. On the other hand, the degradation is not stopped completely since photons with shorter wavelengths (less than 500 nm) are hardly absorbed by the CB.

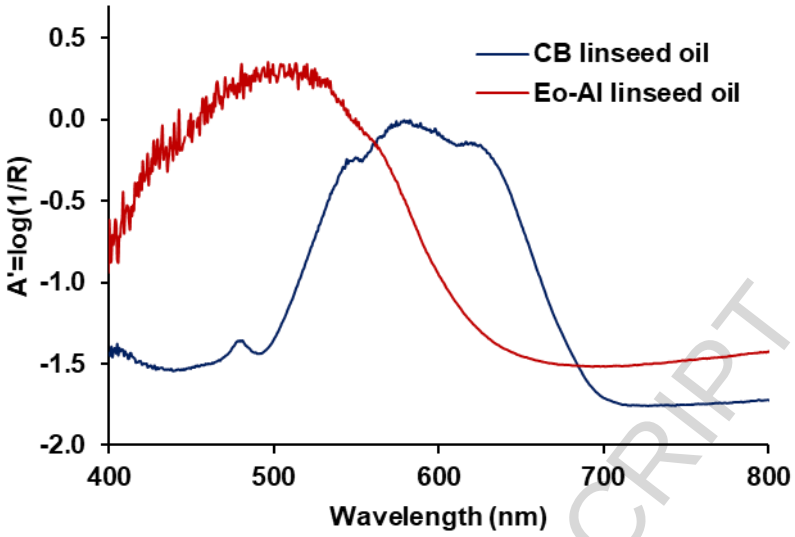

Fig. 7. Pseudo-absorbance (A') spectrum of Eo-Al and CB in linseed oil (unaged).

3.3. FTIR-ATR spectroscopy

With the motivation of providing a further explanation of the color changes due to the light exposure, FTIR-ATR spectra of the eosin lakes and the unaged and aged (192 h) paint reconstructions were recorded on the surface of the paints. The study of these spectra is quite arduous because of the pronounced absorption due to the linseed oil, lead white and cobalt blue components. Therefore, the presence of eosin is not always obvious and only a few of its characteristics bands are observed. The spectra of linseed oil, cobalt blue and lead white are described in greater detail in supplementary information (Fig. S7) in order to identify their characteristic bands.

The recorded FTIR-ATR spectra of the powdered eosin lakes studied in this paper are included in Fig. S8. The FTIR-ATR spectra for the eosin lakes have a characteristic broad band between 3200-2000 cm^{-1} associated with the intermolecular hydrogen bonding and aromatic C-H stretching vibrations. Small differences can be observed in this band based on the conformation

in the lakes previously described [22]. Interestingly, none of the three studied lakes feature a band at 1750 cm^{-1}, indicating that the lactone conformation of the eosin is not (significantly) present. The range between 1600-1200 cm^{-1} corresponds to the asymmetrical and symmetrical stretching modes of the carboxylate. Notice that the two bands around 1450 and 1330 cm^{-1} showed slight differences for Eo-Pb compared with Eo-Al or Eo-Al/K. These differences could be ascribed to the different anchoring position and binding mode of the metals to the eosin molecule and the nature of the different salts used during the synthesis [22]: (i) Eo-Al and Eo-Al/K show similar spectra indicating that the coordination between the metal and the eosin in the lake presents the same conformation (bridge bidentate anchor); however the presence of lead as a metal indicates a differently anchored (H-bonded) complex (ii) Since only Eo-Pb was prepared by precipitation of lead (II) acetate trihydrate, it is possible that the observed difference is also due to a bidentate bridging anchoring mode of the acetate group. Also, the different pattern presented in the spectral range between 1000 and 400 cm^{-1} indicates structural differences among the 3 lakes.

In Fig. 8, the FTIR-ATR spectra obtained after ageing are compared with the spectra of the unaged samples in order to detect differences due to light exposure. The three lakes show a similar aging behavior when mixed with linseed oil (Fig. 8A and Fig. S9A-B).

After aging, some samples (Fig. 8B-C) showed the increase of the band intensity at 1740 cm^{-1}, related to the (C=O) stretching, and the decrease of the intensities at 2920 and 2852 cm^{-1}, related to the CH_2 asymmetric stretching. These changes have been associated with the oxidative degradation of the linseed oil [39] (see Fig. S7).

The spectra of the Eo-Al (Fig. 8) show a general decrease of the intensities of the FTIR absorption bands after light exposure. In the samples where eosin is the only pigment present in

the paint model (Fig. 8A). The bands in the range between 1600-500 cm^{-1} shown a decreased intensity. The band at 1625 cm^{-1} associated to the ν(C=O) from the quinone and the bands at 1330 and 1260 cm^{-1}due to C-C and C-O-C stretching at the xanthene [40] showed a clearly decrease after aging. These changes might be attributed to the structural changes of the molecule under light exposure.

A selection of the FTIR-ATR spectra for samples containing LW and Eo-Al in different ratios show a higher decreased in the bands described above as an evidence of the high photosensitivity of eosin in presence of LW (Fig. 8B-C). When Eo-Al is present in high abundance (Fig. 8B) the spectrum shows a broad band around 1400 cm^{-1} which includes an absorption band of lead white (1390 cm^{-1}) and eosin (1450 cm^{-1}) (see Fig. S7 and S8). After light exposure the intensity of the band around 1400 cm^{-1} clearly diminished its intensity and the band at 1330 cm^{-1} disappears. It is also noticeable that the band at 1570 and the bands around 1000-400 cm^{-1}, previously assigned to the eosin lake, show a decrease in intensity after aging. However, the band at 682 cm^{-1} corresponding to lead white remained unchanged.

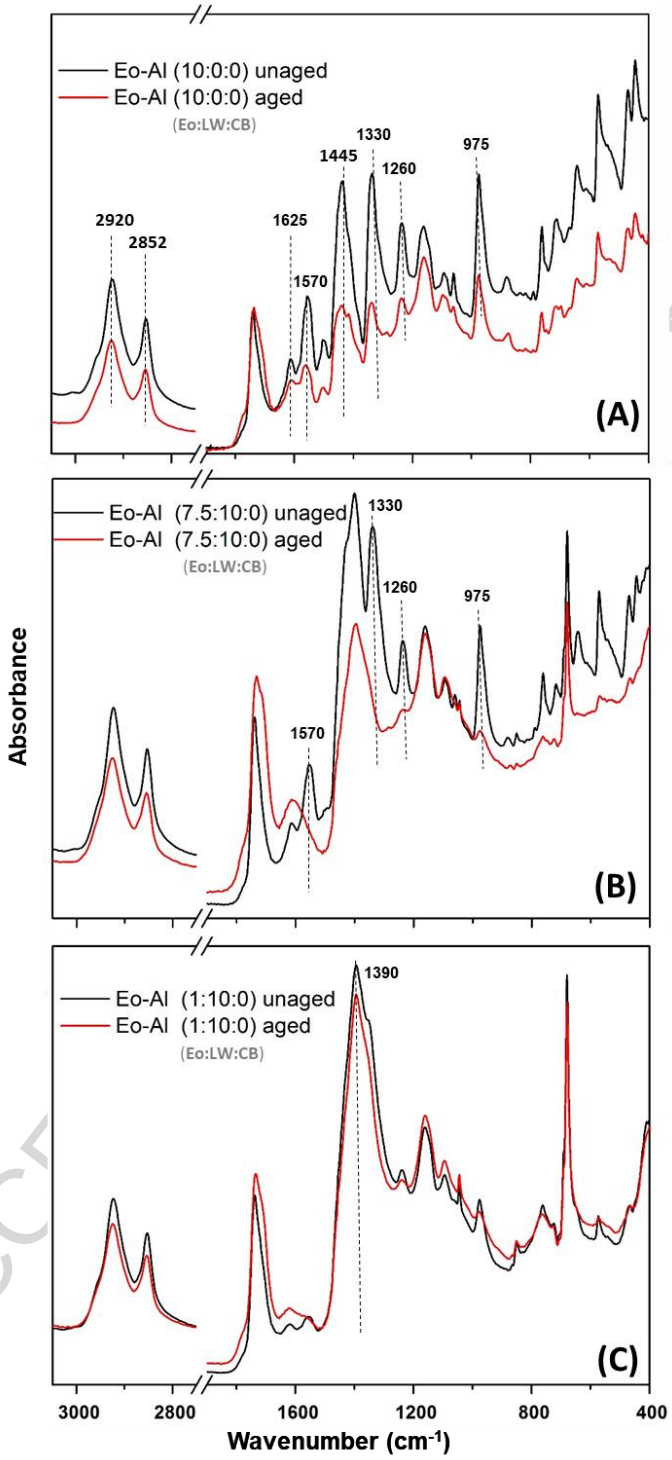

Fig. 8. FTIR-ATR spectra before (black line) and after aging (red line). **(A)** Eo-Al **(B, C)** Eo-Al in combination with different mass ratios of LW. FTIR-ATR spectra were acquired on the paint surface.

The paint model containing the lowest abundance of Eo-Al shows a broad band around 1390 cm^{-1}, characteristic of lead white (Fig. 8C). In this case, a subtle change in band intensity of the shoulder around 1330 cm^{-1} was observed after the aging experiment.

The presence of cobalt blue in the paint models has a weak effect on the FTIR-ATR spectra, since the bands associated with this pigment are between 600 and 400 cm^{-1}. In the paints where cobalt blue and eosin are present, the spectra after aging showed a minor decrease of the bands associated with the degradation of eosin and the linseed oil (Fig. S10), similar to the spectra observed when Eo was the only pigment in the paint (Fig. 8A and Fig. S9).

3.4. Raman spectroscopy

Because the main absorption of Eo-M is around 517 nm, a red laser excitation line (785 nm) was used to record the Raman spectra of eosin in the powders (Fig. S11), surfaces (top layers) (Fig. 9 and Fig. S12) and along the cross sections (Fig. 10) without inducing any degradation of the pigment. Furthermore, it has been demonstrated that a strong fluorescence background, observed during the analysis of eosin, is reduced when a red laser is employed in the analysis [41].

The spectra acquired when the powdered lakes are exposed to red laser light (Fig. S11) match with those obtained in previous studies of eosin [30, 41]. The three Eo-M show similar spectra across the entire range dominated by the bands arise from the xanthene moiety (Table S1).

Raman spectra of two samples containing different ratios of eosin lake and lead white are included in Fig. 9A-B. The data shows that the Raman intensities ascribed to eosin diminish (see Table S1) with light exposure. The spectra of both samples show an increase of the characteristic lead white band at 1051 cm^{-1} after light exposure. The decrease of the intensities and thus the degradation of eosin is more pronounced when the lead white abundance increases in the

mixture. When LW is present in high abundance (Fig. 9B) a single band, which belongs to lead white, remains after light exposure. While the bands previously assigned to the chromophore are not detected, indicating a quasi-total breakdown of the structure of eosin at the surface of the paint model.

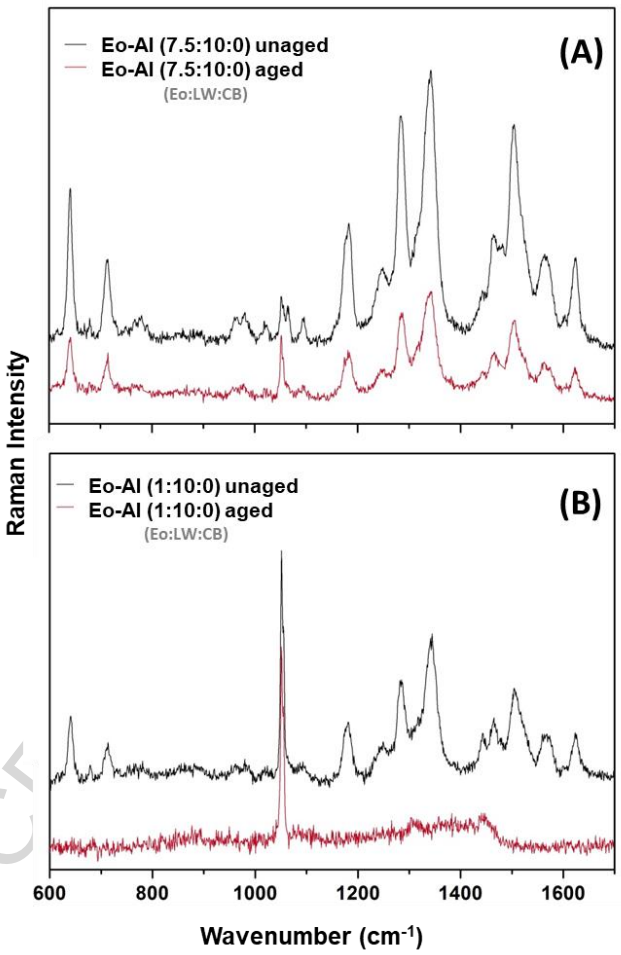

Fig. 9. Raman spectra before (black line) and after aging (red line) of Eo-Al in combination with different ratios of LW. Raman spectra were acquired on the paint surface.

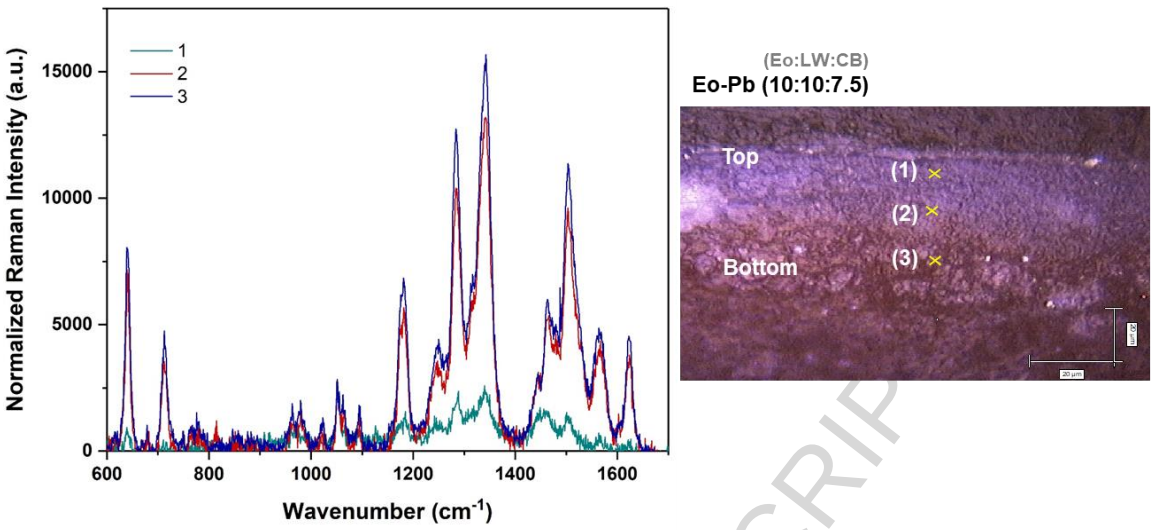

Fig. 10. Raman spectra acquired on the cross section of an aged sample at different depths from the surface. Spectra have been normalized to the CO_3^{2-} band of LW at 1051 cm^{-1}.

Raman results of these aged samples are in accordance with the degradation pattern observed in the FTIR-ATR analysis (Fig. 8), where in the case of the less diluted mixture (Fig. 8B) the degradation of eosin could be readily observed, while in the most diluted mixture, the spectrum was dominated by the contribution from lead white (Fig. 8C).

The effect of cobalt blue in the paint models remains quite unclear, since characteristic Raman bands of the blue pigment could not be observed under the conditions employed. Fig.S12 shows two different samples where the ratio between cobalt blue and eosin remains constant and the only difference is the lead white abundance. When lead white is present in the sample (Fig. S12B) the loss of the Raman intensity is more pronounced after aging, showing that the presence of lead white has a stronger effect over the degradation of the eosin lake.

Raman analysis was also performed on cross section samples showing a clear surface discoloration. The spectra recorded and their corresponding points along the sample are included in Fig. 10. The discoloration observed on the first 10 µm below the surface can be related to the

decrease in Raman intensity of eosin, confirming the (partial) degradation of eosin in the top of the sample. Unfortunately, no spectral differences were found in the samples analyzed by Raman spectroscopy, since the vibrational modes of potential intermediates, previously hypothesized, could be too weak to be detected, or covered by fluorescence effects.

In addition, the green laser (514 nm) was used with the aim of identifying possible photodegradation products of the three eosin powders (data not shown). Analysis reveals that no new bands are registered; therefore, we can conclude that under the studied conditions the green laser does not induce any degradation of the Eosin lakes.

4. Conclusions

The artificial aging of paint models is a useful tool to characterize the discoloration process of eosin lakes and to identify the influence that other pigments have over this process. In order to examine the effect that different pigments may have in the stability of geranium lake, a number of samples were prepared by mixing the three eosin-based lakes synthetized in this study with different ratios of lead white and cobalt blue.

The color changes observed in the present paper have been associated with the degradation of the red lake, likewise the extent of its discoloration might be correlated with the different nature of the pigments present in the paint. On the one hand, samples containing lead white were more affected by the light than the ones with cobalt blue. This can be explained by the translucent nature of lead white: ultraviolet radiation coming in the paint layer is not totally reflected by lead white therefore, the light can cross the paint, leading to an internal light scattering inside the paint causing a strong color change in the paint. On the other hand, cobalt blue absorbs the light in the surface, giving rise a discoloration only in the upper few millimeters of the paint.

However, the partial discoloration observed in samples containing cobalt blue may be due to the fact that cobalt blue reflects at wavelength higher than 650 nm, but also reflects the light around 520 nm. It is this light that is strongly absorbed by eosin and likely destabilizes it. A comparison study between the reflectance spectra and the L* coordinate revealed the impact of the ratios of lead white and cobalt blue are clearly associated with the brightening/darkening of the paint models

The structural differences obtained by FTIR-ATR analysis are directly related with the different discoloration patterns observed by UV-VIS spectroscopy. At the same time, the monitoring of the discoloration via colorimetric measurements allowed us to formulate the hypothesis that different degradation mechanisms may be associated with the nature of the pigments present in the paint. In follow up research involving molecular characterization by mass spectrometry techniques that allow to distinguish between the (subtly) different eosin degradation products, this could be confirmed; detailed results will be presented in a sequel paper to the present. The combination of Raman spectroscopy, OM and SEM-EDX analysis allowed for the correlation of the discoloration along the paint with the degradation of eosin lakes.

The changes observed in this study are in accordance with those obtained from the analysis of Van Gogh's paintings and can offer a better understanding of the discoloration of eosin under light exposure. This study may give an explanation of the changes over the time will help to achieve the possible color used by the artist.

This papers reveals the complexity in the discoloration process of geranium lake due to the numerous factors that can affect its stability. Work is currently in progress on the analysis of the fading process of eosin lakes in the presence of binders and pigments to understand the mutual influence.

Acknowledgements

The authors sincerely acknowledged Dr. Costanza Miliani for sharing information about the synthesis of geranium lake. The authors also acknowledged Dr. Geert van der Snickt and Gert Nuyts for the help with the aging experiments and for carrying out the SEM-EDX measurements respectively.

References

[1] F. Vanmeert, G. Van der Snickt, K. Janssens, Plumbonacrite Identified by X-ray Powder Diffraction Tomography as a Missing Link during Degradation of Red Lead in a Van Gogh Painting, Angew. Chem. Int. Ed. 54 (2015) 3607-3610.

[2] L. Monico, K. Janssens, M. Cotte, L. Sorace, F. Vanmeert, B.G. Brunetti, C. Miliani, Chromium speciation methods and infrared spectroscopy for studying the chemical reactivity of lead chromate-based pigments in oil medium, Microchem. J. 124 (2016) 272-282.

[3] G. Van der Snickt, K. Janssens, J. Dik, W. De Nolf, F. Vanmeert, J. Jaroszewicz, M. Cotte, G. Falkenberg, L. Van der Loeff, Combined use of Synchrotron Radiation Based Micro-X-ray Fluorescence, Micro-X-ray Diffraction, Micro-X-ray Absorption Near-Edge, and Micro-Fourier Transform Infrared Spectroscopies for Revealing an Alternative Degradation Pathway of the Pigment Cadmium Yellow in a Painting by Van Gogh, Anal. Chem. 84 (2012) 10221-10228.

[4] K. Janssens, G. Van der Snickt, F. Vanmeert, S. Legrand, G. Nuyts, M. Alfeld, L. Monico, W. Anaf, W. De Nolf, M. Vermeulen, J. Verbeeck, K. De Wael, Non-Invasive and Non-Destructive Examination of Artistic Pigments, Paints, and Paintings by Means of X-Ray Methods, Top. Curr. Chem. 374 (2016) 81.

[5] M.L. Franquelo, J.L. Perez-Rodriguez, A new approach to the determination of the synthetic or natural origin of red pigments through spectroscopic analysis, Spectrochim. Acta Part A 166 (2016) 103-111.

[6] F. Sabatini, A. Lluveras-Tenorio, I. Degano, S. Kuckova, I. Krizova, M.P. Colombini, A Matrix-Assisted Laser Desorption/Ionization Time-of-Flight Mass Spectrometry Method for the Identification of Anthraquinones: the Case of Historical Lakes, J. Am. Soc. Mass. Spectrom. 27 (2016) 1824-1834.

[7] A. Chieli, J. Sanyova, B. Doherty, B.G. Brunetti, C. Miliani, Chromatographic and spectroscopic identification and recognition of ammoniacal cochineal dyes and pigments, Spectrochim. Acta Part A 162 (2016) 86-92.

[8] I. Degano, P. Tognotti, D. Kunzelman, F. Modugno, HPLC-DAD and HPLC-ESI-Q-ToF characterisation of early 20th century lake and organic pigments from Lefranc archives, Herit. Sci. 5 (2017) 7.

[9] M.d. Keijzer, M.R. van Bommel, M. Geldof, Synthetic organic pigments used by Vincent van Gogh at the end of his lifetime, EU-Artech Symposium on Vincent van Gogh and Contemporaries, Amsterdam, Nederland, 2009.

[10] A. Claro, M.J. Melo, S. Schäfer, J.S. Seixas de Melo, F. Pina, K.J. van den Berg, The use of microspectrofluorimetry for the characterization of lake pigments, Talanta 74 (2008) 922-929.

[11] M. Geldof, M. Keijzer, M. Bommel, K. Pilz, J. Salvant, H. Keulen, Van Gogh's Geranium Lake, in: M. Vellekoop, M. Geldof, E. Hendriks, L. Jansen, A. deTagle (Eds.), Van Gogh's studio practice, Mercatorfonds, Brussels, 2013.

[12] M.R. van Bommel, M. Geldof, E. Hendriks, An investigation of organic red pigments used in paintings by Vincent van Gogh (November 1885 to February 1888), ArtMatters, 3, 2005.

[13] E. Hendriks, L. Jansen, J. Salvant, E. Ravaud, M. Eveno, M. Menu, I. Fielder, M. Geldof, L. Megens, M. Van Bommel, C. Johnson, D. Johnson, A Comparative Study of Vincent van Gogh's Bedroom Series, Studying Old Master Paintings: Technology and Practice. The National Gallery Technical Bulletin 20th Anniversary Conference Postprints, 2010, pp. 237-243.

[14] A. Burnstock, I. Lanfear, K. van der Berg, L. Carlyle, M. Clarke, E. Hendriks, J. Kirby, A comparision of the fading and surface deterioration of red lake pigments in six paintings by Vicent van Gogh with artificially aged paint reconstructions. Preprints of the 14th Triennial Meeting of the ICOM Committee for Conservation, The Hague, 2005, pp. 459-466.

[15] B.H. Berrie, Y. Strumfels, Change is permanent: thoughts on the fading of cochineal-based watercolor pigments, Herit. Sci. 5 (2017) 30.

[16] T. Hayashi, A. Kazlauciunas, P.D. Thornton, Dye conjugation to linseed oil by highly-effective thiol-ene coupling and subsequent esterification reactions, Dyes Pigm. 123 (2015) 304-316.

[17] B.A. van Driel, P.J. Kooyman, K.J. van den Berg, A. Schmidt-Ott, J. Dik, A quick assessment of the photocatalytic activity of TiO_2 pigments — From lab to conservation studio!, Microchem. J. 126 (2016) 162-171.

[18] G. Oster, G.K. Oster, G. Karg, Extremely long-lived intermediates in photochemical reactions of dyes in non-viscous media, J. Chem. Phy. 66 (1962) 2514-2517.

[19] K. Kimura, T. Miwa, M. Imamura, The Radiolysis and Photolysis of Methanolic Solutions of Eosin. II. The Photo-Debromination of Eosin in an Alkaline Solution, Bull. Chem. Soc. Jpn. 43 (1970) 1337-1342.

[20] A. Seret, A. Van De Vorst, The photochemistry of the semi-oxidized form of eosin Y and rose bengal in aqueous sodium dodecylsulphate solutions, J. Photochem. Photobiol. A Chem. 43 (1988) 193-206.

[21] M. Clarke, M. Witlox, J.H. Townsend, A. Stijnman, Historically accurate reconstructions of artists' oil painting materials, in: M. Clarke, J.H. Townsend, A. Stijnman (Eds.), Art Technological Source Research study group: Approaching the Art of the Past: Sources & Reconstructions., Archetype Publications, London, 2005, pp. 53-59.

[22] C. Anselmi, D. Capitani, A. Tintaru, B. Doherty, A. Sgamellotti, C. Miliani, Beyond the color: A structural insight to eosin-based lakes, Dyes Pigm. 140 (2017) 297-311.

[23] E. Kirchner, I. van der Lans, F. Ligterink, M. Geldof, A. Ness Proano Gaibor, E. Hendriks, K. Janssens, J. Delaney, Digitally reconstructing van Gogh's Field with Irises near Arles part 2: Pigment concentration maps, Color Res. Appl. DOI: 10.1002/col.22164.

[24] M. Geldof, L. Steyn, Van Gogh's Cobalt Blue, , in: M. Vellekoop, M. Geldof, E. Hendriks, L. Jansen, A. deTagle (Eds.), Van Gogh’s studio practice, Mercatorfonds, Brussels, 2013.

[25] A. Claro, M.J. Melo, J.S. Seixas de Melo, K.J. van den Berg, A. Burnstock, M. Montague, R. Newman, Identification of red colorants in van Gogh paintings and ancient Andean textiles by microspectrofluorimetry, J. Cult. Herit. 11 (2010) 27-34.

[26] N. Eastaugh, Pigment Compendium: A Dictionary and Optical Microscopy of Historical Pigments, Butterworth-Heinemann, 2008.

[27] Commission Internationale de L'Eclairage, Control of damage to museum objects by optical radiation, CIE 157. ISBN 3901906274, Vienna, Austria, 2004.

[28] A. Alvarez-Martin, S. Trashin, M. Cuykx, A. Covaci, K. De Wael, K. Janssens, Photodegradation mechanisms and kinetics of Eosin-Y in oxic and anoxic conditions, Dyes Pigm. 145 (2017) 376-384.

[29] K. Kimura, T. Miwa, M. Imamura, Photochemical debromination of eosin in basic methanolic solution, Chem. Commun. (London) (1968) 1619-1621.

[30] S.A. Centeno, C. Hale, F. Carò, A. Cesaratto, N. Shibayama, J. Delaney, K. Dooley, G. van der Snickt, K. Janssens, S.A. Stein, Van Gogh's Irises and Roses: the contribution of chemical analyses and imaging to the assessment of color changes in the red lake pigments, Herit. Sci. 5 (2017) 18.

[31] J.E. Fieberg, P. Knutas, K. Hostettler, G.D. Smith, "Paintings Fade Like Flowers": Pigment Analysis and Digital Reconstruction of a Faded Pink Lake Pigment in Vincent van Gogh's Undergrowth with Two Figures, Appl. Spectrosc. 71 (2017) 794-808.

[32] D. Saunders, J. Kirby, Light-induced colour changes in red and yellow lake pigments, in: A. Roy (Ed.), National Gallery Technical Bulletin, National Gallery Publications, London, vol 15, 1994, pp. 79-97.

[33] J. Kirby, D. Saunders, Fading and color change of prussian blue: methods of manufacture and the influence of extenders, in: A. Roy (Ed.), National Gallery Technical Bulletin, National Gallery Publications, London, vol 25, 2004, pp. 73-99.

[34] R.L. Feller, R.M. Johnston-Feller, C. Bailie, Determination of the Specific Rate Constant for the Loss of a Yellow Intermediate during the Fading of Alizarin Lake, JAIC 25 (1986) 65-72.

[35] Z.C. Koren, Chromatographic and colorimetric characterizations of brominated indigoid dyeings, Dyes Pigm. 95 (2012) 491-501.

[36] E.M. Arbeloa, C.M. Previtali, S.G. Bertolotti, Photochemical study of Eosin-Y with PAMAM dendrimers in aqueous solution, J. Lumin. 180 (2016) 369-375.

[37] L.I. Grossweiner, E.F. Zwicker, Transient Measurements of Photochemical Processes in Dyes. I. The Photosensitized Oxidation of Phenol by Eosin and Related Dyes, J. Chem. Phy. 34 (1961) 1411-1417.

[38] L. Pronti, A.C. Felici, M. Ménager, C. Vieillescazes, M. Piacentini, Spectral Behavior of White Pigment Mixtures Using Reflectance, Ultraviolet—Fluorescence Spectroscopy, and Multispectral Imaging, Appl. Spectrosc. 0 (2017) 1-10.

[39] E. Marengo, M.C. Liparota, E. Robotti, M. Bobba, Monitoring of paintings under exposure to UV light by ATR-FT-IR spectroscopy and multivariate control charts, Vib. Spectrosc, 40 (2006) 225-234.

[40] L. Wang, A. Roitberg, C. Meuse, A.K. Gaigalas, Raman and FTIR spectroscopies of fluorescein in solutions, Spectrochim. Acta, Part A, 57 (2001) 1781-1791.

[41] N.G. Greeneltch, A.S. Davis, N.A. Valley, F. Casadio, G.C. Schatz, R.P. Van Duyne, N.C. Shah, Near-Infrared Surface-Enhanced Raman Spectroscopy (NIR-SERS) for the Identification of Eosin Y: Theoretical Calculations and Evaluation of Two Different Nanoplasmonic Substrates, J. Phys. Chem. A 116 (2012) 11863-11869.

Figure Captions

Fig. 1. Optical microscopy of resin-embedded paint cross sections before (left) and after (right) ageing. UV illumination from the top in all cases. The samples (A-E) correspond to five paint models containing different mass ratios of Eo-Pb, lead white and cobalt blue. (A) 10:0:0; (B) 7.5:10:0; (C) 1:10:1; (D) 10:0:7.5; (E) 10:10:7.5.

Fig. 2. Optical photographs of the surface of Eo-Al paint models before (left) and after (right) ageing. Numbers correspond to the sample codes given in Table 1. (For comparison, equivalent images for the Eo-Pb and Eo-Al/K paint models are included in Fig. S3-4).

Fig. 3. Comparison of influence of the complex metal (Al, Pb or Al/K) in the total color change, measured in units of ΔE*, against aging time. **(A)** Paint models containing only Eo-M; **(B)** paint models containing mixtures of Eo-M and CB; **(C)** Paint models containing mixtures of Eo-M and LW. **(E-F)** ternary Eo-M, LW and CB mixtures.

Fig. 4. CIELAB diagrams of paint models consisting of **(A)** Eo-Al/K and lead white and **(B)** Eo-K/Al and cobalt blue mixtures showing changes in redness (a*) and yellowness (b*) during the aging experiment. The color used for the symbols represent the color of each sample during light exposure. **(C)** and **(D)** represent total observed color change of ΔE*, during the aging experiment for the same set of samples. Mixtures based on Eo-Pb and Eo-Al lakes instead of Eo-Al/K showed similar results.

Fig. 5. CIELAB diagrams of paint models containing different mass ratios of Eo-Al or Eo-Pb, lead white and cobalt blue (A) and (B) showing the changes in redness (a*) and yellowness (b*) during the aging experiment. The color used for the symbols represent the color of each sample after light exposure. (C) and (D) represent the total color change ΔE* during the aging experiment for the same set of samples. Mixtures based on Eo-Al/K showed similar results.

Fig. 6. **(A-D)** Selection of the diffuse reflectance UV-VIS spectra of paint models before and after aging. **(E)** Represents the variation of the L* (lightness/darkness value) for the same samples.

Fig. 7. Pseudo-absorbance (A') spectrum of Eo-Al and CB in linseed oil (unaged).

Fig. 8. FTIR-ATR spectra before (black line) and after aging (red line). **(A)** Eo-Al **(B, C)** Eo-Al in combination with different mass ratios of LW. FTIR-ATR spectra were acquired on the paint surface.

Fig. 9. Raman spectra before (black line) and after aging (red line) of Eo-Al in combination with different ratios of LW. Raman spectra were acquired on the paint surface.

Fig. 10. Raman spectra acquired on the cross section of an aged sample at different depths from the surface. Spectra have been normalized to the CO_3^{2-} band of LW at 1051 cm^{-1}.

Highlights

- The different effect of lead white and cobalt blue on the discoloration of eosin lakes was studied.
- Structural differences (FTIR-ATR) were related with different discoloration patterns (UV-VIS)
- Raman, OM and SEM-EDX correlate the discoloration of the paint with the degradation of eosin lakes
- Discoloration in the paint reconstructions was linked to Van Gogh's paintings